

A new fast velocity-diffusion modelling for impurity transport in integrated edge plasma simulation

K. Shimizu *, T. Takizuka, H. Kawashima

Japan Atomic Energy Agency, 801-1 Mukoyama, Naka-shi, Ibaraki-ken 311-0193, Japan

Abstract

A fast velocity-diffusion model, which applies to an impurity Monte–Carlo (MC) code, such as IMPMC, is newly developed. The algorithm significantly reduces the computational time, especially in detached plasma, its speed attains more than 100 times faster than the conventional MC method. The performance of IMPMC is further optimized on the massive parallel computer. Thereby the IMPMC is combined with a so-called divertor code, and a self-consistent modelling of divertor plasma and impurity transport is successfully achieved. The integrated code, SONIC (SOLDOR/NEUT2D/IMPMC) is characterized by treatment for kinetic effects and complicated dissociation process of methane. As initial simulations with SONIC, the dynamic evolution of X-point MARFE in JT-60U is investigated. Neutral carbons chemically sputtered from the dome in the private region can deeply penetrate into the main plasma and are subsequently ionized/recombined near the X-point. The resultant carbon ions cause large radiation during MARFE phase.

© 2007 Elsevier B.V. All rights reserved.

PACS: 52.25.Vy; 52.40.Hf; 52.55.Fa; 52.65.Pp

Keywords: Divertor modelling; Impurity transport; Chemical sputtering; MARFE; JT-60U

1. Introduction

For compatibility of high confinement core plasma with strong radiative divertor, it is necessary to establish the control method for impurity retention in the divertor region. A number of 2D multi-fluid divertor code have been developed, e.g. B2 [1], EDGE2D [2], UEDGE [3] and used for investigation of the impurity and plasma transport. The impurity transport is solved as one species of fluids

in their codes. We have proceeded to another approach for impurity modelling [4]. Monte–Carlo (MC) approach is superior to the fluid model from the aspect of flexibility of modelling [5]. Interactions between impurities and walls, and kinetic effects can be easily included into the modelling. Furthermore only MC model can practically deal with the complicated dissociation process of methane [6]. Therefore some elaborate Monte–Carlo Impurity transport codes, e.g. DIVIMP [7], IMPMC [4], MCI [8], have been developed to investigate impurity transport in more detail. With the use of the MC code, however, the impurity transport has been studied under fixed parameter of background

* Corresponding author. Fax: +81 029 270 7468.

E-mail address: shimizu.katsuhiro@jaea.go.jp (K. Shimizu).

plasma to date. For a consistent analysis, we are aiming at coupling of IMPMC code into a 2D divertor code (SOLDOR/NEUT2D) [9]. This task is very difficult due to a significant amount of computational time and noise in MC calculation.

When a conventional MC algorithm is employed for scattering process in velocity space, the impurity ions must be traced with a time step Δt much shorter than the slowing-down time τ_s . It follows that the MC code requires a huge amount of computational time, especially in case of detached plasma ($n_e \sim 1 \times 10^{20} \text{ m}^{-3}$, $T_e = T_i \sim 1 \text{ eV}$) because of extremely short slowing-down time, typically, $\tau_s \sim 7 \times 10^{-9} \text{ s}$ for C^{3+} . We develop a new diffusion model using analytical solution of Langevin equations, which can significantly reduce the computational time. Thereby combining the SOLDOR/NEUT2D code and the IMPMC code becomes possible. By using the early phase of this unified code, SONIC, we carry out the simulation of dynamic evolution of the X-point MARFE observed in JT-60U.

2. New diffusion model

The impurity ions diffuse in the velocity space by Coulomb collisions with the plasma ions, and the spatial diffusion parallel to the magnetic field line arises from the change of parallel velocity due to collisions. The IMPMC code treats correctly the velocity-space diffusion (VD model) for this process. The similar MC code, DIVIMP, employed the spatial diffusion model (SD model) before [7]. A random displacement $\Delta s = \sqrt{2D_{\parallel}}\Delta t \cdot r_G$ in the parallel direction s is given at every time step. Here $D_{\parallel} = v_{\text{th}}^2 \cdot \tau_s$ is the parallel diffusion coefficient and r_G is a normal random number. Comparing these two models, we pointed out that the SD model could not be applied for the plasma where the characteristic time of parallel motion (Δt_{tr}) is comparable to collision time [10]. This issue was also discussed in Ref. [11].

We reformulate these processes, i.e. the relation between the velocity and spatial diffusion processes. These processes are described by the following Langevin equations:

$$v^{n+1} = v^n + F_{\parallel}\Delta t/m_z - (v^n - V_f)\Delta t/\tau_s + \{(\Delta v^2)\Delta t\}^{1/2}r_G, \quad (1)$$

$$s^{n+1} = s^n + v^n\Delta t, \quad (2)$$

where the superscript n denote time step number, v is the parallel velocity, s is the parallel position, m_z

is the mass of impurity ion, F_{\parallel} is the parallel force on impurity ion, V_f is the parallel flow velocity of plasma, and $\langle\Delta v^2\rangle\Delta t$ is the mean square deviation of velocity diffusion during a time step. As the analytical solution of Langevin equations, the mean (μ) and the standard deviation (σ^2) of the parallel velocity (v) and the parallel position (s) are obtained, as follows:

$$\mu_v(t) = v_0 \exp(-t/\tau_s) + v_{\infty}\{1 - \exp(-t/\tau_s)\}, \quad (3a)$$

$$\sigma_v^2(t) = 1/2\{1 - \exp(-2t/\tau_s)\}\langle\Delta v^2\rangle\tau_s, \quad (3b)$$

$$\mu_s(t) = v_{\infty}t + (v_0 - v_{\infty})\tau_s\{1 - \exp(-t/\tau_s)\}, \quad (4a)$$

$$\sigma_s^2(s) = 1/2\{2t/\tau_s - 3 + 4\exp(-t/\tau_s) - \exp(-2t/\tau_s)\}\langle\Delta v^2\rangle\tau_s^3, \quad (4b)$$

where v_0 is the parallel velocity at $t = 0$ and v_{∞} is defined by $v_{\infty} = V_f + F_{\parallel}\tau_s/m_z$.

In the new diffusion model, the position and the velocity of a test particle at the time t can be chosen from the normal distributions with two normal random numbers, r_{G1} and r_{G2} .

$$s(t) = \mu_s(t) + \sigma_s(t) \cdot r_{G1}, \quad (5)$$

$$v(t) = \mu_v(t) + \sigma_v(t) \cdot r_{G2}. \quad (6)$$

We examine the new diffusion model by comparing with a conventional MC model (VD model). The following parameters are used; the number of test particles is $N = 5000$, $\Delta t = \tau_s/20 = 0.01$, $\tau_s = 0.2$, $V_f = 0$, $F_{\parallel} = 0$, $v_0 = 2.0$, and $\langle\Delta v^2\rangle\Delta t = 0.025$. The bold line represents the evolving distribution of parallel position (Fig. 1(a)) and parallel velocity (Fig. 1(b)) obtained by the conventional MC model. Each dotted line represents the distribution calculated by the new diffusion model with only a single time step. The agreement is quite well, not only for $t \gg \tau_s$ (diffusion phase) but also for $t \leq \tau_s$ (free flight phase). When we treat the non-uniform system, we should keep the time step shorter than the transit time ($\Delta t \ll \Delta\tau_{\text{tr}}$). In the case of the slowing-down time being comparable to the transit time (in the most case of attached plasma parameter), the VD model should be employed for this diffusion process. Present code switches between the VD model and new diffusion model, for each test particle as appropriate according to the ratio between the transit time and the slowing-down time.

The computational time can be significantly reduced by this new algorithm. In a case where 5000 test particles are traced during 1 ms in the typical detached divertor plasma ($n_e \sim 1 \times 10^{20} \text{ m}^{-3}$, $T_e \sim 1 \text{ eV}$), it takes 1 h to perform the simulation

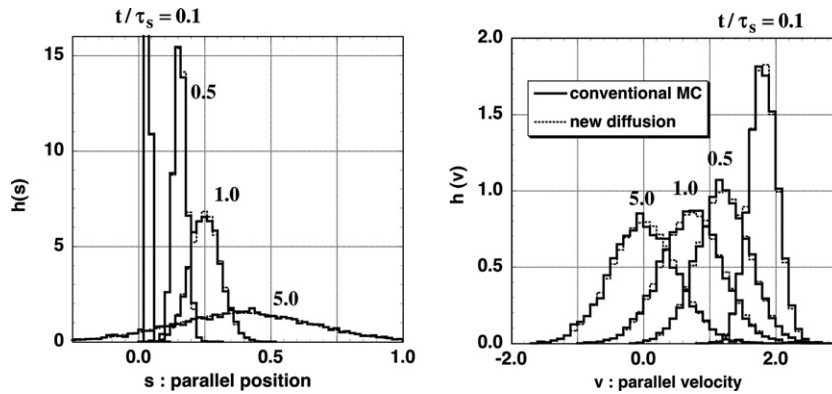


Fig. 1. Distribution of parallel position and parallel velocity. Solid line represents the simulation with the conventional model (VD model). Dotted line represents the distribution calculated by the new diffusion model.

with the conventional method ($\Delta t = 1/20 \cdot \tau_s$) whereas it takes only 12 s to do it with the new algorithm ($\Delta t = 10^{-6}$ s) on SGI ALTIX 3900.

3. SONIC code

In the Japan Atomic Energy Agency, a divertor code system that consists of fluid codes, Monte-Carlo codes and particle simulation codes has been comprehensively developed [12]. As main part of this project, we have successfully developed a self-consistent code of divertor plasma and impurity transport, i.e. combining the SOLDOR/NEUT2D code [9] and the IMPMC code [4]. The key feature of this unified code, SONIC, is to incorporate the elaborate impurity Monte-Carlo code. In general, development of such code is difficult because of computational time and noise in MC calculation. We resolve this problem by introducing the new diffusion model. The IMPMC performance is further optimized by using Message Passing Interface (MPI) on the massive parallel computer, SGI ALTIX 3900. An IMPMC calculation is performed for 30 ms plasma duration to obtain carbon distribution in a steady state, every 100 steps of SOLDOR with a typical time step of 1×10^{-6} s. To reduce MC noise, 50,000 test particles are employed for each carbon source. The radiation loss and ionization loss are calculated at every iteration step of SOLDOR code using carbon density distributions for each charge state calculated with IMPMC code. (iteration step: We adopt the Newton-Raphson method for solving non-linear fluid equations in SOLDOR.)

The IMPMC code includes the modelling of the physical sputtering and chemical sputtering as generation mechanism of carbon impurities. Taking

account of physical sputtering yields [13] and incident fluxes of deuterium ions onto the target plates, the sputtered outfluxes are determined self-consistently. In addition, the chemical sputtering is induced by the neutral and ion fluxes onto the target plates and the wall. The incident fluxes of ions (D^+) and neutral particles (D^0 , D_2) are calculated with SOLDOR and NEUT2D codes, respectively.

The modelling of dissociation process of methane and dynamics of dissociation products (CD_3^+ , CD_3 , CD_2^+ , etc.) was treated in the previous IMPMC simulations [6]. However, these complicated dissociation processes of CD_4 are not taken into account in the present work for simplicity. We treat chemically sputtered CD_4 as a carbon C with a low energy (~ 1 eV) as used in other divertor codes. However we try to take into consideration the feature of the dissociation of CD_4 . It is characterized by presence of neutral hydrocarbons, which are produced by the dissociative recombination. Some of the neutral hydrocarbons return to the wall when the velocity directions are randomized at the neutralization. As a result, the generation rate of C^+ ions from methane changes from 0.1 at target plates to 0.5 at private wall, which depends on the location of sputtering [6]. Taking this effect in the dissociation model, the chemical sputtering yield is effectively reduced from the standard value of 0.05 [14,15] to 0.02. Furthermore, a displacement of ~ 1.5 cm in poloidal plane from ionization point is randomly added to simulate the cross-field movement of neutral hydrocarbon.

4. Simulation results

The simulation is carried out for the typical parameter of the JT-60U neutral-beam heated

divertor plasma ($I_p = 1.5$ MA, $B_T = 3$ T, $P_{NB} = 5$ MW). In this discharge, the X-point MARFE occurred by a strong gas puffing. The heat flux and the particle flux from the core edge ($\rho/a = 0.95$) are specified, $Q_i = Q_e = 2$ MW, $\Gamma_i = 0.25 \times 10^{22} \text{ s}^{-1}$. We assume $D_{\perp} = 0.25 \text{ m}^2/\text{s}$ for the anomalous particle diffusion coefficient and $\chi_{\perp}^i = \chi_{\perp}^e = 1 \text{ m}^2/\text{s}$ for the anomalous thermal diffusivities. The recycling coefficient at the divertor plates and walls is set to 1.0 for both ion and neutral particles. The albedo for neutral particles at the pumping port is specified so as to satisfy pumping speed of $S_{\text{pump}} = 26 \text{ m}^3/\text{s}$ [16]. The diffusion coefficient for carbon impurity is assumed to be $1 \text{ m}^2/\text{s}$ [4]. The self-sputtering is not included in the present simulation.

The steady state calculation without gas puffing is performed at first. The attached divertor plasma is obtained and the radiation of carbon peaks near both strike points as shown in Fig. 2(a). Next, a strong gas puff of $\Gamma_{\text{puff}} = 0.8 \times 10^{22} \text{ s}^{-1}$ is introduced to the above attached plasma. The evolution of the carbon radiation profile is shown in Fig. 2(b)–(d). The radiation peaks move away from the strike point and shift slightly upstream in the partially detached plasma (Fig. 2(b)). The region with high radiation power extends from the strike point up to near the X-point along the separatrix. In the fully detached plasma, the radiation peaks shift to near the X-point as shown in Fig. 2(c). Finally, the peaks move into the main plasma and the single peak stays at the X-point as shown in Fig. 2(d). These evolutions of radiation profile are basically the same as that observed in JT-60U experiments with a strong gas puffing [17]. The detailed comparison with the experiment is for the future work. Fig. 2(d) shows that a remarkable narrow region appears inside the separatrix near the X-point. It is characterized by the extremely high density ($4 \times 10^{20} \text{ m}^{-3}$), and low temperature ($2 \sim 3$ eV) in spite of the core edge. Such plasma profiles during MARFE phase are also presented in the simulations with B2/EIRENE in the recent review paper [18], and other simulations in references therein.

In the calculation of impurity transport with IMPMC, the collisions between impurity ions are neglected. This test particle approximation is valid when $Z_{\text{eff}} < 1 + \sqrt{2m_i/m_e} \approx 1.6$ [19], where m_i is the mass of background plasma. The Z_{eff} varies from 1.1 to 1.5 in the divertor plasma of attached case, while Z_{eff} in the divertor plasma of completely detached case is reduced to 1.1. Thus the test parti-

cle approximation can be applied to the present simulations.

The contamination of carbon impurities into the main plasma is investigated with the IMPMC results. In the attached plasma, the ionization of neutral carbon physically sputtered takes place mainly near the target plates (Fig. 3(a)). The carbon sputtered chemically from the targets is also ionized near the target plates (not shown). On the other hand, the carbons sputtered chemically from the private wall are ionized in the private region and no neutral carbon is ionized in the main plasma as shown in Fig. 3(b). In the fully detached plasma, the carbons are ionized upstream in the SOL. The 5% of sputtered carbon from the dome is ionized in the main plasma because the electron temperature in the private region is low around 1–2 eV. Such carbons cause the high radiation power of $\geq 5 \text{ MW/m}^3$ near the X-point during the MARFE phase.

5. Summary and future work

We develop a new diffusion model for parallel motion and scattering process with the MC scheme. This new algorithm can significantly reduce the computational time of MC code. Thereby we successfully develop a coupling code of SOLDOR/NEUT2D and IMPMC as a self-consistent modeling of divertor plasma and impurity transport. Initial simulations with the unified code, SONIC basically reproduce the dynamic evolution of X-point MARFE observed in JT-60U. It is found that the radiation near the X-point during MARFE originates in neutral carbons chemically sputtered from the private region.

The electron energy loss term is included consistently as the interactions between plasma and impurity in the present SONIC, but the electron particle source/loss term caused by ionization/recombination of impurities is neglected temporarily. The improvement in the modelling is in progress. We are also equipping the model of the complicated dissociation process of methane. Neutral-neutral collisions and impurity-impurity collisions are neglected respectively in NEUT2D code and IMPMC code. The assumption for IMPMC is barely justified in the present calculations, but it becomes inapplicable to the attached plasma as electron density decreases and/or electron temperature increases in the core edge. In order to expand the application of the SONIC code, we intend to

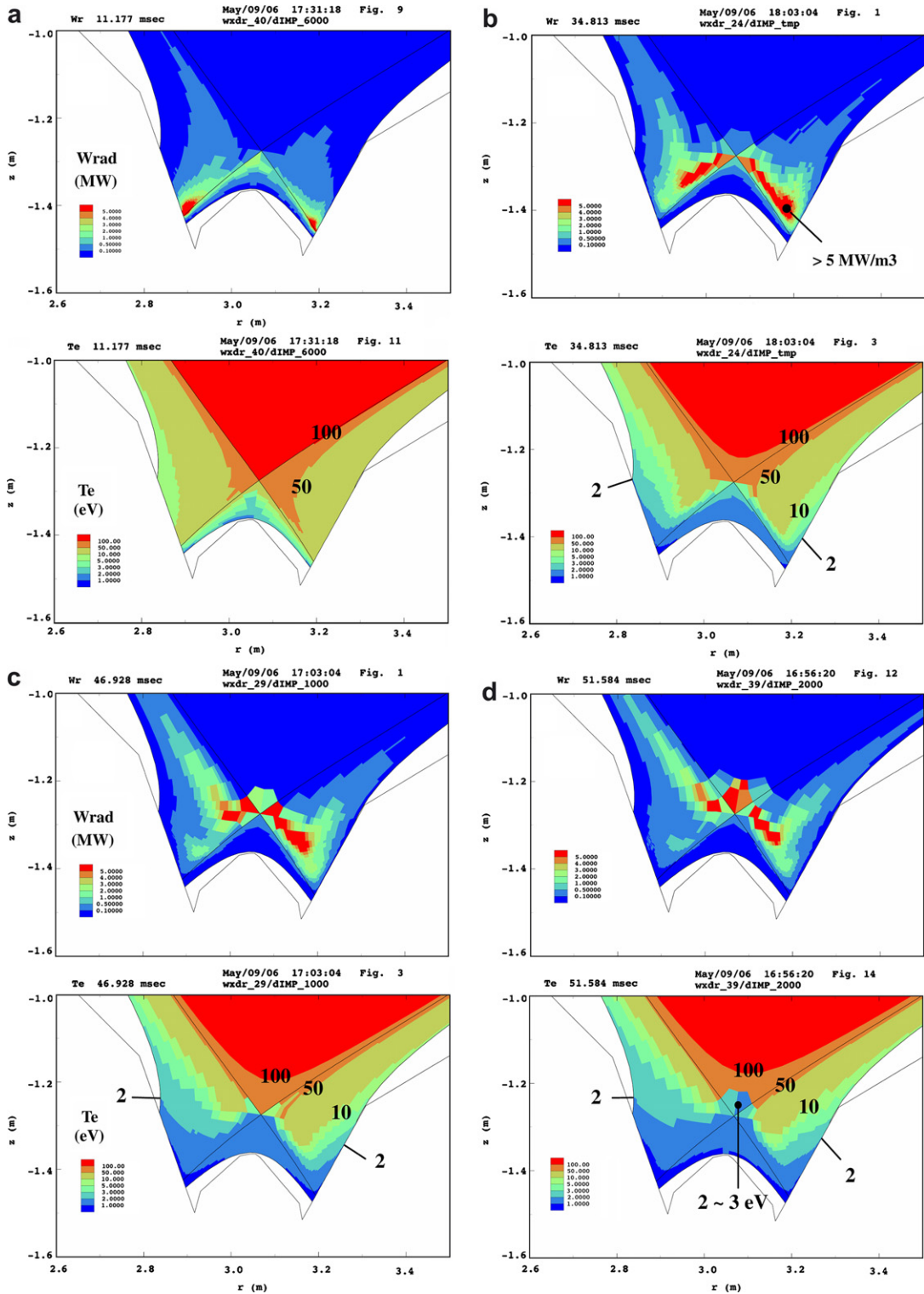


Fig. 2. Time evolution of radiation profile calculated with SONIC (SOLDOR/NEUT2D/IMPIC) code. (a) Attached plasma in a steady state before gas puffing. (b) Partially detached plasma. (c) Fully detached plasma. (d) X-point MARFE. The strong gas puffing leads to a sequential change from (a) to (d).

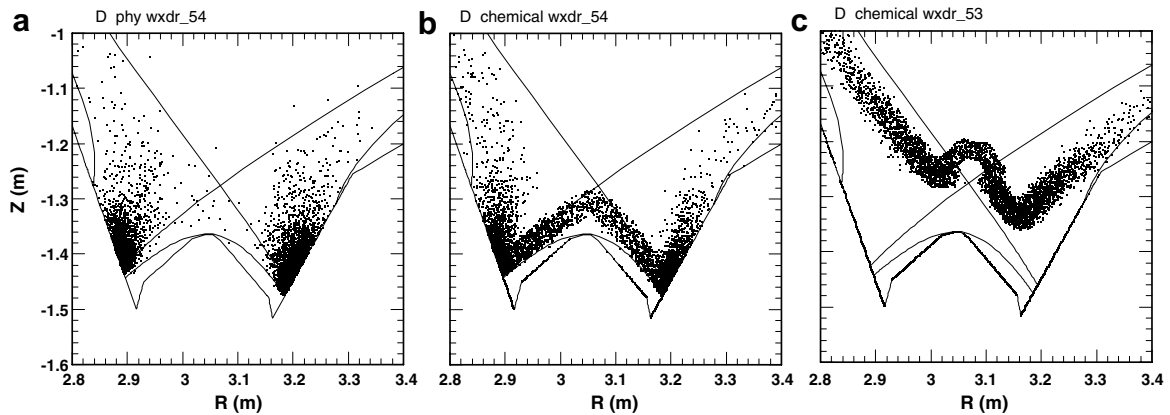


Fig. 3. Ionization points of carbon atoms: (a) physically sputtered from the target plates in attached plasma, (b) chemically sputtered from the dome in attached plasma, and (c) chemically sputtered from the dome in fully detached plasma with a X-point MARFE. Each simulation is carried out with 50,000 test particles. The ionization points of 10,000 test particles are plotted in each figure.

include these collision effects in MC modelling as a future task. The SONIC code, which contains impurity kinetic effects and consistent interactions with plasma and impurity, is expected to clarify the generation and transport of impurities, e.g. erosion and redeposition of carbon target plates.

Acknowledgements

The authors would like to thank Drs S. Konoshima and T. Nakano for fruitful discussions about the radiation and plasma parameter in JT-60U experiments. They are also indebted to Drs T. Ozeki and M. Kikuchi for their continuous encouragement. This work is partly supported by the Grant-in-Aid for Scientific Research of Japan Society for the Promotion of Science.

References

- [1] R. Schneider et al., *J. Nucl. Mater.* 196–198 (1992) 810.
- [2] R. Simonini et al., *J. Nucl. Mater.* 196–198 (1992) 369.
- [3] T.D. Rognien et al., *J. Nucl. Mater.* 196–198 (1992) 347.
- [4] K. Shimizu et al., *J. Nucl. Mater.* 220–222 (1995) 410.
- [5] K. Shimizu et al., *J. Nucl. Mater.* 241–243 (1997) 167.
- [6] K. Shimizu et al., *Plasma Physics and Controlled Nuclear Fusion Research 1994 (Proc. 15th Int. Conf. Seville, 1994)*, Vol. 3, IAEA, Vienna, 1996, 431.
- [7] P.C. Stangeby, J.D. Elder, *J. Nucl. Mater.* 196–198 (1992) 258.
- [8] T.E. Evans et al., *J. Nucl. Mater.* 266–269 (1999) 1034.
- [9] K. Shimizu et al., *J. Nucl. Mater.* 313–316 (2003) 1277.
- [10] K. Shimizu, T. Takizuka, Impurity transport code based on Monte Carlo techniques (IMPMC), Tech. Mtg on ITER Divertor Physics Design, Garching, 1994.
- [11] P.C. Stangeby, J.D. Elder, *Nucl. Fusion* 35 (1995) 1391.
- [12] H. Kawashima, et al., *Plasma Fusion Res.* 1 (2006) 031 http://www.jspf.or.jp/PFR/PFR_articles/pfr2006_06.html.
- [13] J. Roth et al., *Suppl. J. Nucl. Fusion* (1991) 64.
- [14] T. Nakano et al., *Nucl. Fusion* 42 (2002) 689.
- [15] J.V. Philips et al., *J. Nucl. Mater.* 313–316 (2003) 354.
- [16] H. Kawashima et al., *J. Nucl. Mater.*, these Proceedings, doi:10.1016/j.jnucmat.2007.01.127.
- [17] S. Konoshima et al., *J. Nucl. Mater.* 313–316 (2003) 882.
- [18] R. Schneider et al., *Contrib. Plasma Phys.* 46 (2006) 2.
- [19] Yu. L. Igitkhanov, *Contrib. Plasma Phys.* 28 (1988) 477.